

1 Driving singing behaviour in 2 songbirds using multi-modal, 3 multi-agent virtual reality

4 Leon Bonde Larsen^{1*}, Iris Adam², Gordon J. Berman³, John Hallam¹, Coen P.H.
5 Elemans²

*For correspondence:
lelar@mmmi.sdu.dk

6 ¹University of Southern Denmark, SDU-Biorobotics, Odense, Denmark; ²University of
7 Southern Denmark, Department of Biology, Odense, Denmark; ³Emory University,
8 Department of Biology, Atlanta GA, USA

10 **Abstract** Interactive biorobotics provides unique experimental potential to study the
11 mechanisms underlying social communication but is limited by our ability to build expressive
12 robots that exhibit the complex behaviours of birds and small mammals. An alternative to
13 physical robots is to use virtual reality (VR). Here, we designed and built a modular, audio-visual
14 virtual reality environment that allows online, multi-modal, multi-agent interaction for social
15 communication. We tested this system in songbirds, which provide an exceptionally powerful
16 and tractable model system to study social communication. We show that zebra finches
17 (*Taeniopygia guttata*) communicating through the VR environment exhibit normal call timing
18 behaviour, males sing female directed song and both males and females display high-intensity
19 courtship behaviours to their mates. These results suggest that the VR system provides a
20 sufficiently natural environment to elicit normal social communication behaviour. Furthermore,
21 we developed a fully unsupervised online song motif detector and used it to manipulate the
22 virtual social environment of male zebra finches based on the number of motifs sung. Our VR
23 setup represents a first step in taking automatic behaviour annotation into the online domain
24 and allows for animal-computer interaction using higher level behaviours such as song. Our
25 unsupervised acoustic analysis eliminates the need for annotated training data thus reducing
26 labour investment and experimenter bias.

28 Introduction

29 Social communication involves multiple individuals that interact in networks, typically through
30 multi-modal signals, such as vision and sound. Deciphering the mechanisms underlying social com-
31 munication requires experimental manipulation of the complex multi-modal interactions within
32 the social network. The field of interactive biorobotics provides unique experimental possibilities
33 by letting animals interact with robots to understand, for example, mating behaviours (*Patricelli*
34 *et al., 2006; Reaney et al., 2008; Partan et al., 2011; Klein et al., 2012*), the underlying rules of
35 shoaling behaviour (*Marras and Porfiri, 2012; Polverino et al., 2013; Kopman et al., 2013; Bonnet*
36 *et al., 2016*) and communication signals (*Partan et al., 2010; Benichov et al., 2016*). This approach
37 is limited by our ability to build expressive robots that exhibit complex behaviours. What passes
38 for an expressive robot is species and hypothesis dependent, but many animals will readily accept
39 a robot as part of their social network (*Michelsen et al., 1992; Halloy et al., 2007; de Margerie et al.,*
40 *2011; Romano et al., 2017*). Building and controlling a small expressive robot might be possible in

41 some cases (*Simon et al., 2019*) but is often not a viable solution for small model animals due to
42 the mechanical and computational complexity involved in fully mimicking natural behaviours.

43 An alternative to physical robots is to use virtual reality (VR) (*Dombeck and Reiser, 2012*), de-
44 fined as "a real or simulated environment in which a perceiver experiences telepresence" (*Steuer,*
45 *1992*). Current VR setups used in larval zebra fish (*Ahrens et al., 2012*), fruit flies (*Reiser and Dickin-*
46 *son, 2008*) and mice (*Harvey et al., 2009*) virtualise the position of the agent in the environment by
47 providing computer-generated visual feedback. The visual stimulus is generated by measuring the
48 real-world movements of the agent and apply the same translation to its virtual position (*Reiser*
49 *and Dickinson, 2008; Harvey et al., 2009; Ahrens et al., 2012; Kaupert et al., 2017; Stowers et al.,*
50 *2017; Cong et al., 2017*). To provide a sufficiently natural virtual environment to interact with and
51 drive the behaviour of an agent, the system needs to be fast enough to analyse, compute and
52 generate the virtual environment within the perceptual real-time of the agent. We refer to this
53 requirement as online operation (*Larsen et al., 2021*). Studying social communication in a virtual
54 environment in most cases also requires multi-modal signals, such as vision and sound and inter-
55 action between multiple agents (*Rychen et al., 2021*), but so far VR environments have, to the best
56 of our knowledge, only been used to study single agents. Taken together, to experimentally ma-
57 nipulate social communication, we need a multi-agent VR setup that supports online manipulation
58 of multi-modal signals.

59 A potentially excellent system for studying social behaviour in a VR context is vocal interaction
60 in songbirds. Zebra finches (*Taeniopygia guttata*) live in societies and form interactive networks
61 through calls (*Zann, 1996; Ter Maat et al., 2014; Anisimov et al., 2014; Benichov et al., 2016; Elie*
62 *and Theunissen, 2016*). The male song is a learned complex behaviour and is part of the mating
63 ritual where both visual and auditory cues play crucial roles in the natural behaviour (*Zann, 1996*).
64 To situate a zebra finch in virtual reality requires at least sound and vision but is likely also in-
65 fluenced by gaze (*Davidson and Clayton, 2016*) and orientation relative to other agents (*Ljubičić*
66 *et al., 2016*). Previous work has shown that zebra finches interact vocally with an immobile phys-
67 ical decoy providing audio from a built-in speaker (*Benichov et al., 2016; Benichov and Vallentin,*
68 *2020*) and are physically attracted to more life-like actuated zebra finch robots (*Simon et al., 2019*).
69 Furthermore, adult finches can recognize and discriminate between conspecifics from live video
70 feeds (*Galoch and Bischof, 2006, 2007*) and sing song to still images (*Adret, 1997*) or live video
71 feeds of females (*Ikebuchi and Okanoya, 1999; Adret, 1997*). Also, juvenile males can learn song
72 from video and audio playback of a tutor (*Chen et al., 2016; Carouso-Peck and Goldstein, 2019*).
73 Finally, online perturbation of virtual auditory environments can drive active error correction of
74 song (*Sober and Brainard, 2009; Hoffmann et al., 2012*). Taken together, these studies suggest
75 that zebra finches allow studying social behaviour in a VR context. However, no multi-agent VR
76 setup currently exists that supports online, multi-modal manipulation of social communication in
77 zebra finches, and we do not know if zebra finches exhibit normal vocal behaviour when placed in
78 VR environments.

79 Results

80 We present a modular, audio-visual VR environment able to experimentally manipulate social com-
81 munication. Our system allows for online, multi-modal, multi-agent interaction and focuses on
82 songbirds. Our VR setup is implemented in a box placed inside a cage and the cage is placed in a
83 sound attenuating isolator box. We record and present a high-speed (60 fps) visual environment
84 through a teleprompter system that allows direct eye contact and ensures a realistic visual perspec-
85 tive of the video (Fig 1A). The cage has two perches with presence sensors (Fig 1A); one in front of
86 the teleprompter screen (front perch) and one behind an opaque divider that does not allow visual
87 contact with the screen (back perch). Connecting two VR setups provides the visual impression that
88 the other animal is located 20 cm away (Fig 1B). We furthermore record the acoustic environment
89 and present audio from a speaker located behind the teleprompter to provide the cue that sound
90 and video have the same spatial origin. Data from all sensors is streamed on a network, translated

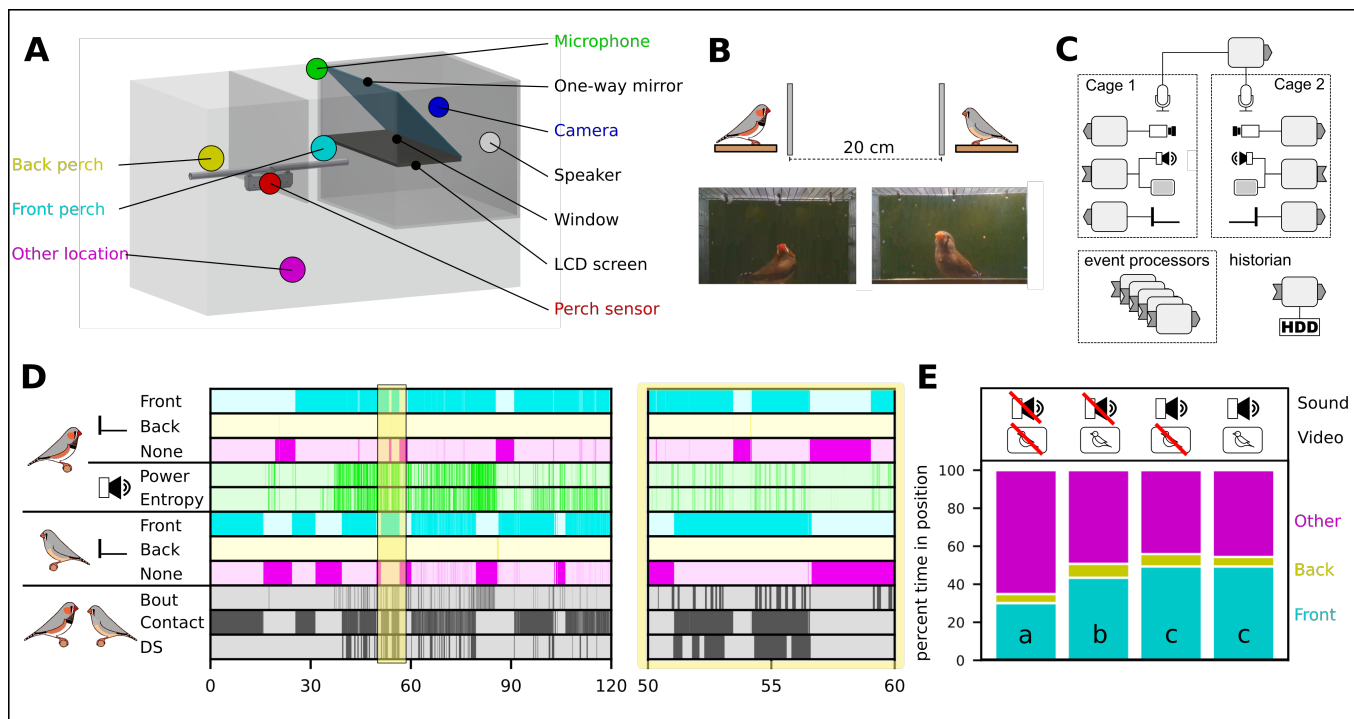


Figure 1. A modular multi-agent multi-modal VR setup for social communication in birds. **A:** The cage equipped with the VR setup and an opaque divider. On the front perch the bird is able to see the screen, while not when it sits on the back perch. **B:** Connecting two VR setups provides the visual impression of the other animal being twice the distance between the bird and the camera away; in this case 20cm. **C:** The distributed hardware architecture of the setup based on *Larsen et al. (2021)*. See Methods for more detail. **D:** Perch and acoustic events produced during two hours of communication through the VR setup and a 10-minute zoom of the area with yellow overlay. For complex event definitions see main text. **E:** The perch preference in four different experimental conditions. Different letters denote significant difference (two-proportion z-test, 1 % significance level, $n=24$).

91 online into events using cloud-based event processing (*Larsen et al., 2021*) and is captured for of-
 92 fline processing by a node connected to storage (historian, Fig 1C). This modular and distributed
 93 design allowed for scaling of individual parts of the system (e.g., to add sensors or online software
 94 analyses) and can be extended to connect multiple VR setups.

95 Event Processing (*Cugola and Margara, 2012*) was used to represent onset and offset of be-
 96 havioural features and event streams from multiple producers were combined to form new events
 97 (Fig 1D). The position of a single bird generated three different events for absence/presence on the
 98 front or back perch or other location (Fig 1D, cyan, yellow and magenta lines). When connecting
 99 two VR setups with one bird in each cage, a visual contact event was defined as both birds perched
 100 in front of the screen and thus able to see each other. To detect and identify vocal signals, the au-
 101 dio stream from the male was analysed online (see methods) to generate events based on power
 102 and entropy threshold-crossings (Fig 1D, green lines). A bout of song was detected by combining
 103 power and entropy with hysteresis thus suppressing most noise. Finally, a directed song (DS) event
 104 was generated when bout and contact were active at the same time (Fig 1D, bottom line) in other
 105 words, when a male was singing while both male and female were sitting on the front perch.

106 To investigate the animals' motivation for social interaction through the VR setup, we measured
 107 the perch preference of twelve pair-bonded male-female couples in four different audio-visual
 108 modality combinations of speaker/screen on and off. Our data showed that birds spent signifi-
 109 cantly more time on the front perch when one modality (either sound or video) from the other
 110 bird was on (Fig 1E). When both video and audio modalities were on, birds also spent more time
 111 on the front perch than video-only but not when compared to live audio (two-proportion z-test,
 112 1 % significance level, $n=24$). This demonstrates that the birds were attracted to both audio and

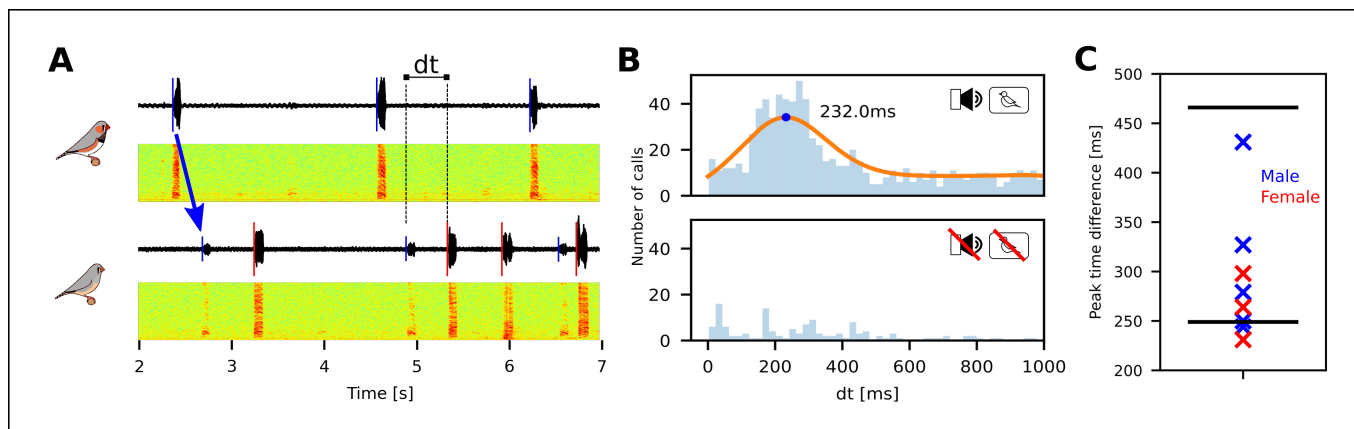


Figure 2. Zebra finches communicating through the VR setup exhibit natural call timing behaviour. **A:** Sound oscillograms and spectrograms for the stack calls of a male and a female communicating through VR setups. Detected onsets are indicated by vertical lines on the oscillograms. The arrow denotes that the playback of the male call can be seen in the recording of the female. We measure the time dt from playback to answer. **B:** Histogram of the elapsed time between the playback of the mate's call until next call in one pair. The peak of the kernel density estimate is marked. Bottom plot shows a histogram of time differences for the same pair with the system off. **C:** Summary showing the peak for all 8 birds. The black lines show the range of values reported in (Benichov et al., 2016).

113 visual signals of another individual supplied by the virtual reality system.

114 To demonstrate that the VR setup provided a sufficiently natural environment for social com-
 115 munication, we exploited two key behaviours in communication between pair-bonded individuals:
 116 call timing and directed song. Coordinated call production between partners is a well described
 117 behaviour in birds, where it is thought to influence pair-bond maintenance and mate guarding (Elie
 118 et al., 2010). Zebra finches show time-locked call behaviour using two types of calls: Tet and
 119 stack calls (Ter Maat et al., 2014). Both are short, low power vocalizations used when the birds
 120 are physically close together (Zann, 1996; Elie and Theunissen, 2016). We quantified the call tim-
 121 ing of stack calls between established pair bonded couples communicating through our VR envi-
 122 ronment (Fig 2A) and identified calls using a supervised random forrest classifier (see Methods).
 123 With both audio and visual modalities on, the delay from hearing a call to producing one was uni-
 124 modally distributed (Fig 2B) with a peak delay at 291 ms (median: 271 ms, range: 231-431 ms,
 125 $N=8$, Fig 2BC). This data is consistent with call timing delay measured between free-moving pairs in
 126 colonies ($\bar{191}$ ms (Ter Maat et al., 2014), 249-466 ms (Benichov et al., 2016) and 68-283 ms (Anisi-
 127 mov et al., 2014)). Because calls were synchronized and contingent on the call of the mate, we
 128 conclude that the birds displayed natural call timing behaviour through the VR setup.

129 Next, we studied whether the VR setup provided a sufficiently natural environment for males
 130 to exhibit natural singing behaviour to their virtual mate. Male zebra finches sing both to females
 131 (directed song, DS) and not directed towards any particular conspecific (undirected song, US) (Zann,
 132 1996). The song consists of introductory notes and a stereotyped sequence of syllables, called the
 133 motif, that is often repeated several times to form a song bout (Zann, 1996; Sossinka and Böhner,
 134 1980). Although the DS and US motif consist of the same syllable sequence, several key acoustic
 135 features are different between DS and US. The DS motif is delivered faster and is preceded by
 136 more introductory notes (Jarvis et al., 1998). It also has more repetitions of the motif in each bout,
 137 increased sequence stereotypy (Sossinka and Böhner, 1980) and DS syllables exhibit less variation
 138 in the fundamental frequency of harmonic stacks (Kao et al., 2005).

139 We studied five established pair-bonded couples communicating through our VR environment
 140 and we isolated candidate DS events as the simultaneous occurrence of bout and contact events,
 141 i.e., when both animals were perched in front of the screen and the male was vocalizing. The
 142 video segments of potential DS events were subsequently scored for accompanied behaviour by
 143 experienced observers (IA, CPHE). All (5/5) males sang directed song to their virtual mates and

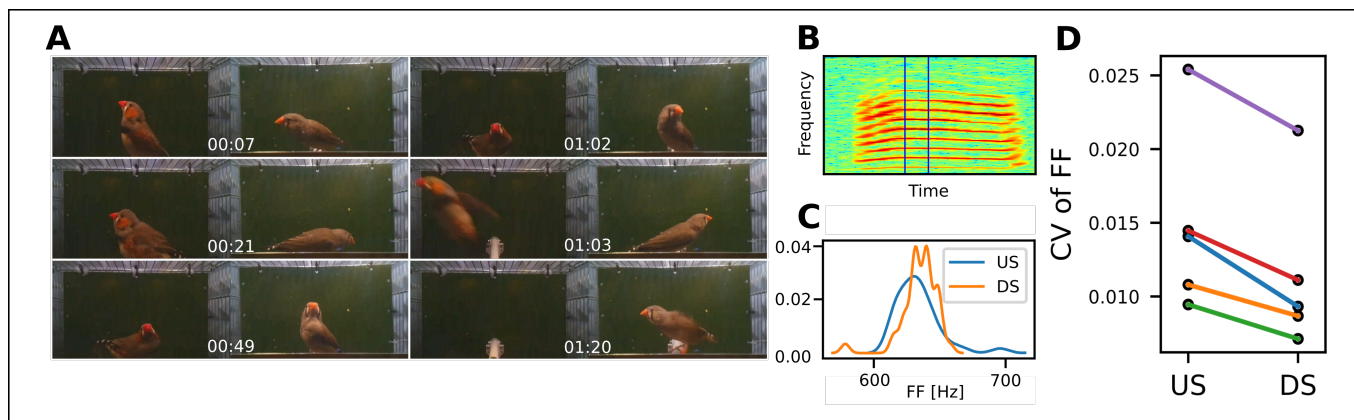


Figure 3. Adult male zebra finches sing directed song to their mate through the VR system. A: Male (left) and female (right) displaying behaviours associated with directed song. The full video is available in the supplementary materials (Movie M1). **B:** Spectrogram of a stack call used to estimate fundamental frequency. The vertical lines indicate the part of the syllable used to estimate fundamental frequency **C:** Kernel density estimates for the fundamental frequency of the syllable above based on 30 renditions with the system on (DS) and 30 with the system off (US). **D:** The Coefficient of Variance of the fundamental frequency is significantly lower when the VR system is on (Wilcoxon signed rank test, 5 % significance level, n=5) indicating DS.

144 displayed courtship behaviours, such as fluffing, beak wipes and jumping, that are indicative of
145 DS (Fig 3A; Movie M1) at high intensity. The coefficient of variance of the fundamental frequency
146 (Fig 3BC) was significantly lower (Wilcoxon signed rank test, 5 % significance level, n=5, Fig 3D) when
147 the VR system was on compared to off further indicating DS. Taken together our data strongly
148 suggest that all males sang DS to their virtual mates.

149 In summary, call timing between individuals was comparable to that of freely communicating
150 animals and males sang DS to their virtual mates, which showed that our VR system provided a
151 sufficiently natural environment for multi-modal, multi-agent social communication in songbirds.

152 A final crucial component in the design of an online VR system is the ability to manipulate an
153 agent's environment and thereby drive its behaviour within its perceptual real-time. When zebra
154 finch males sing DS to a female, they typically habituate to its presence, which leads to a reduction
155 in the number of motifs per minute (Jarvis et al., 1998). In experiments requiring extended periods
156 of DS and/or a high number of motifs, this effect is typically countered by introducing novel females
157 to reinvigorate the male (Jarvis et al., 1998; So et al., 2019). Here we aimed to drive DS behaviour
158 and increase the number of produced motifs by presenting different virtual females based on the
159 online measured song performance of the male.

160 Driving song behaviour based on song performance requires online detection of the stereo-
161 typed syllable sequence, i.e., the motif. Therefore we developed a novel, unsupervised online mo-
162 tific detector (see Methods). The detector is based on dimensionality reduction of feature vectors
163 generated from the spectrogram of sound segments (Fig 4A-E). Training of the model was based
164 on 60,000 feature vectors per animal, each representing a segment of sound. The feature vectors
165 were embedded in a 2D space using t-distributed Stochastic Neighbor Embedding (Maaten and
166 Hinton, 2008) and the watershed transform (Meyer, 1994) was used to cluster the space into a be-
167 haviour map (Berman et al., 2014). Next, we computed the transition probability matrix between
168 all syllables in the training data (Fig 4H) and used it to detect the most stereotyped sequence of syl-
169 lables by starting at the globally most likely transition and following the path of locally most likely
170 transitions (Fig 4H). In all the males, this path contained a cycle that we defined as the motif of the
171 individual and it was confirmed by experienced observers (IA, CPHE) to be the correct motif.

172 Next, we extended the method to detect motifs online (Fig 5A). We detected syllable events
173 by analysing the audio stream and post-embedding the sound segments into the previously com-
174 puted 2D space (Fig 5B). Syllable events were then collected in sequence events that were screened
175 for ordered subsets of the motif (see Methods) to create the motif event (see example in Fig 5C).

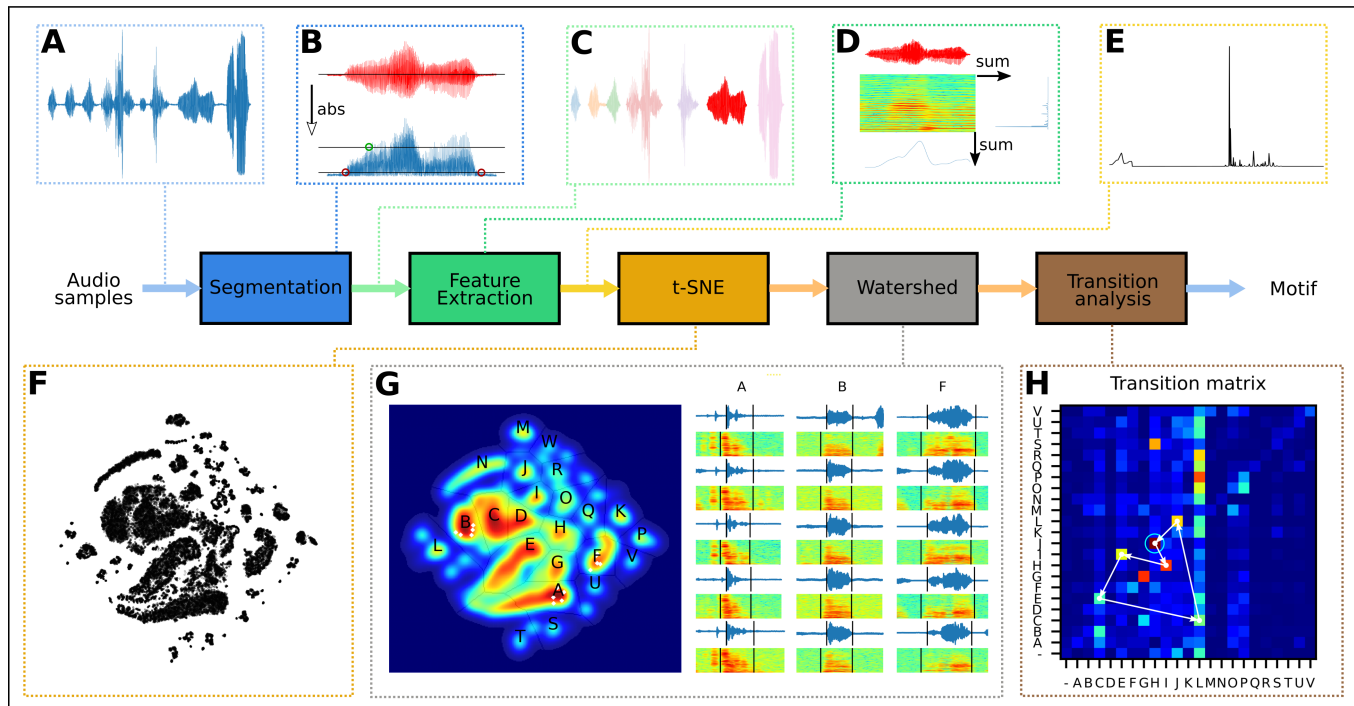


Figure 4. Unsupervised training of motif detector pipeline. **A:** The raw sound signal is received as a continuous stream. **B:** When the absolute value of the samples crosses the high threshold, we search back and forth for onset and offsets based on crossing of the low threshold. **C:** The segmented signal. **D:** A spectrogram of the sound is generated and two vectors are computed by summing the rows and columns, respectively. **E:** The two vectors are normalised and concatenated to a 746-dimensional feature vector. **F:** Dimensionality reduction of 60k feature vectors into a 2D space shows that sound segments cluster together. **G:** Regions of stereotyped sounds are labelled. Examples of randomly picked sounds from three different regions are indicated by white dots on the density plot and with oscillograms and spectrograms on the right. Each column is a different region. **H:** The most common song motif is extracted by forming the transition probability matrix and following the most likely transitions forming a loop. The loop represents the most stereotyped sequence and is defined as the motif.

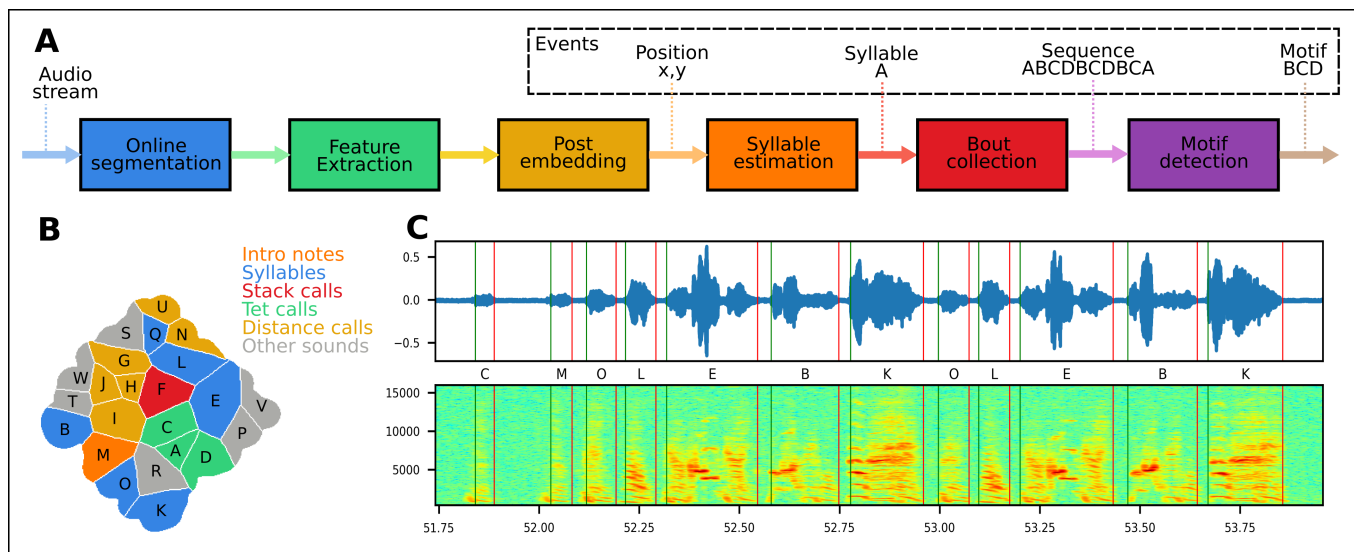


Figure 5. Pipeline for online analysis and event generation. **A:** The pipeline for online analysis uses the methods described in fig. 4A-E for segmentation and feature extraction. The resulting feature vector is post-embedded in the 2D space and classified based on which region it falls within. Syllables are collected in sequences and screened for motifs. **B:** The behaviour map annotated manually based on sample sound segments from each region **C:** Song spectrogram with vertical lines indicating onset (green) and offset (red) events of automatically detected syllables. The letters indicate the class of the syllable.

176 The entire process was parallelised to achieve online detection.

177 Next, we exposed males to one minute audio-visual recordings of one female in an excited state
 178 from the DS experiments, as long as motifs were detected (see Methods). After three minutes
 179 without motif detection, we switched to the audio-visual recordings of another female. Driving
 180 the behaviour over two hours, males sang significantly more motifs (Wilcoxon signed rank test,
 181 5 % significance level, $n=9$) compared to the control period (Fig 6AB). To confirm that the birds
 182 sang DS motifs, we computed the CV of FF in a motif syllable containing a harmonic stack. The
 183 CV was significantly lower during the driving period compared to the control period (Wilcoxon
 184 signed rank test, 5 % significance level, $n=6$), which strongly suggest that the males sang DS to the
 185 virtual females (Fig 6C). Taken together, our VR system made the birds sing more directed motifs
 186 in two hours compared to undirected motifs in the control, thus demonstrating the ability to drive
 187 directed song behaviour.

188 Discussion

189 We present a VR environment to study social communication that allows online, multi-modal, multi-
 190 agent interaction. Zebra finches communicating within the modular VR environment emitted calls
 191 that were synchronized and contingent on the call of the mate with response latencies as in real
 192 life situations (Benichov et al., 2016; Ter Maat et al., 2014; Anisimov et al., 2014). Furthermore,
 193 our data show that males exhibited high-intensity courtship behaviour and sang directed song to
 194 their virtual females. To detect DS events, we used an easily implemented definition of DS as song
 195 that occurs while the birds had visual contact. Previous studies also defined DS as song when
 196 the male was singing oriented towards a conspecific female (Adret, 1997; Chen et al., 2016), but
 197 did not confirm this classification by further acoustic analysis such as decreased DS motif dura-
 198 tion (Jarvis et al., 1998), or decreased variation in the fundamental frequency of harmonic stacks
 199 in DS syllables (Kao et al., 2005). Ikebuchi and Okanoya (1999) classified each song rendition as
 200 either directed or undirected based on dance behaviour but did not indicate their criteria for this
 201 classification. Using both behavioural and acoustic analysis we confirmed that song elicited under
 202 our definition was indeed DS. Taken together, these data strongly suggest that the VR environment

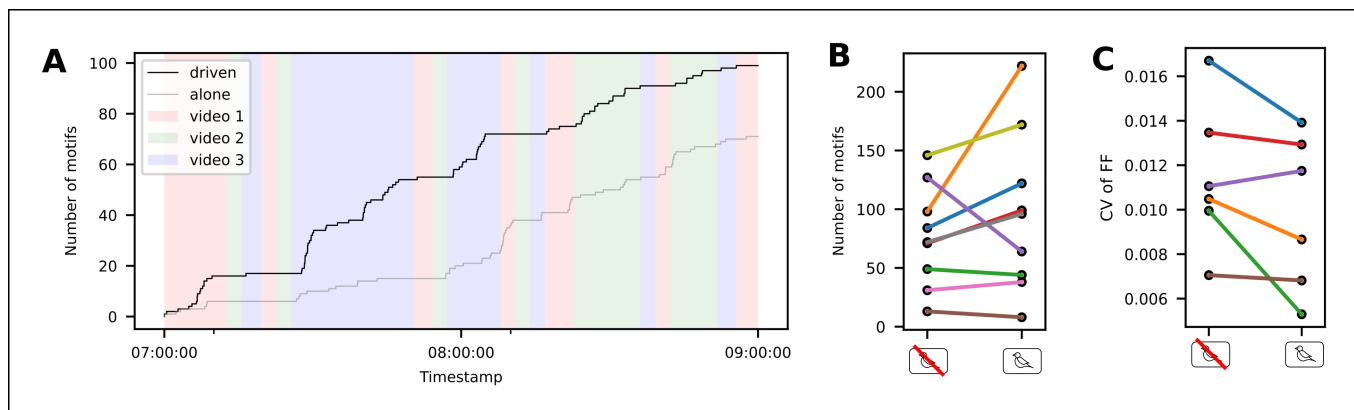


Figure 6. Number of directed motifs can be increased with the help of online motif detection. A: Cumulative sum of detected motifs for one bird during a two-hour period of driving the behaviour by switching virtual female individuals and the same two hours on the following day without video. Background colours show which video was playing during that time. Videos change dynamically based on number of motifs. **B:** The number of motifs sung was significantly higher (Wilcoxon signed rank test, 5 % significance level, $n=9$) during the two hours with video compared to the two-hour control without video demonstrating that the video drives them to sing more. **C:** The coefficient of variance for the fundamental frequency was significantly lower (Wilcoxon signed rank test, 5 % significance level, $n=6$) during the two hours with video compared to the two-hour control confirming that they sing directed song to the video.

203 is sufficiently realistic to elicit the full spectrum of courtship behaviours.

204 We present and implemented a syllable-based unsupervised audio classifier which we think
205 will be widely applicable in bioacoustics. Unsupervised clustering methods have been used in the
206 analysis of vocalisations (*Tchernichovski et al., 2000*) but are typically based on a few dozen acous-
207 tic features. A more data-driven approach is to use spectrograms directly as high dimensional
208 features (*Kollmorgen et al., 2020*), which however imposes extensive computational costs. Here,
209 we compressed the spectrograms to arrive at a manageably sized feature vector thereby keep-
210 ing computational costs low. Especially for stereotyped behaviours, unsupervised methods like
211 t-SNE (*Maaten and Hinton, 2008*) excel because clusters of repeated behaviours stand out from
212 noise (*Berman et al., 2014*). Furthermore, we parallelized a variation of the post-embedding algo-
213 rithm described in *Berman et al. (2014)* to achieve online classification. Lastly, we could determine
214 each individual's motif in an unsupervised way by assuming only that the motif is the most re-
215 peated syllable string, thus exploiting the fact that zebra finch song is highly stereotyped. Our
216 unsupervised method eliminates the need for annotated training data and thereby reduce labour
217 investment and the risk for experimenter bias.

218 Our setup represents a first step in taking automatic behaviour annotation into the online do-
219 main. We used events to represent behaviour and event-processing and microservices to achieve
220 online capabilities (*Larsen et al., 2021*). Several studies have demonstrated the power of online
221 processing in closed loop assays in neuroscience (*Grosenick et al., 2015; Nourizonoz et al., 2020*),
222 to manipulate pitch in songbirds (*Lohr et al., 2003; Brumm and Slabbekoorn, 2005; Riedner and*
223 *Adam, 2020*) or to provide virtual reality (*Ahrens et al., 2012; Reiser and Dickinson, 2008; Harvey*
224 *et al., 2009*). Those studies take advantage of computationally attractive features, such as action
225 potentials or acoustic features, to allow near real time system response. Our approach is slower
226 but allows system response to target higher levels of behavioural organisation, such as syllables
227 or motifs in the audio domain. The limiting factor is the ability to infer online the behaviour of the
228 animal, in other words to parallelise and optimise algorithms for behaviour annotation.

229 Our VR system is modular and can be extended to multiple setups or to add more sensors, ac-
230 tuators, and computational units. We expect our online, modular setup to be applicable to other
231 species of social birds and mammals. We deliberately based the setup on cheap distributed com-
232 puters, free and open-source software, and cloud computing to ease the reuse of hardware and
233 software modules in other projects, and make it easier for multiple developers to contribute. The

234 distributed architecture complicates the system and increases the minimum latency, but allows
235 it to scale linearly, makes it easier to maintain, and makes it resilient to single node failures. The
236 system can be deployed anywhere with network and thereby enables global-scale social commu-
237 nication experiments. VR setups situated around the globe could thus be connected and allow for
238 unique long-term communication experiments between labs that are physically far apart.

239 **Methods**

240 **The VR setup**

241 The VR-setup was built on the teleprompter principle, where a slanted one-way mirror allows the
242 camera to record the bird through the mirror while the bird sees the reflection of a screen below
243 (Fig 1A).

244 A microphone is placed outside the cage above the perch in front of the screen while the rest
245 of the system is placed inside a painted wooden box placed in the cage. The one-way mirror is
246 constructed from a sheet of 3 mm transparent acrylic plexiglass coated by 0.02 mm silver one-way
247 film with 70 % light admittance and 99 % reflectance.

248 The screens are trichromatic 7" LCD displays in 800x480 pixel resolution. Although birds pos-
249 sess at least tetrachromatic or even pentachromatic vision (*Emmerton, 1983*), previous studies
250 showed that males sing when presented with live video of conspecific females on trichromatic
251 screens (*Adret, 1997; Ikebuchi and Okanoya, 1999; Galoch and Bischof, 2006*). However, critical to
252 eliciting courtship behaviour was the use of 100 Hz screens (*Ikebuchi and Okanoya, 1999; Galoch
253 and Bischof, 2006*) that are above the flicker-frequency of birds (*Emmerton, 1983; Nuboer et al.,
254 1992*) or non-flickering liquid-crystal displays (LCD). Therefore, we decided to use 60 Hz LCD screens
255 that present slower, but continuous, flicker-free images to the birds. The video is recorded with a
256 Raspberry Pi Camera V2 in 800x480 pixel resolution at 60 frames per second (fps) and streamed
257 to the network from a Raspberry Pi 3. The video delay was measured by simultaneously turning
258 on an LED in both boxes and recording a video with an external camera showing both the LED and
259 the screen. By counting the number of frames from the local LED turns on to the remote LED from
260 the other box can be seen on the screen the delay can be calculated. This delay was measured to
261 383 ms (23 frames at 60 fps).

262 The audio playback comes from a 1.5 W mini-speaker placed behind the mirror and had to
263 be slightly attenuated (-6dB) to avoid acoustic feedback. The sound was recorded and streamed
264 from a multi-channel recording array (*Andreassen et al., 2014*) using Knowles FG23329-PO7 micro-
265 phones. The recording equipment is not part of the developed VR setup and it could be replaced
266 by any system capable of streaming audio. The audio delay was measured by making a loud sound
267 (with a clicker) in one box and timing the difference between that signal in one box and the version
268 played back in the other box. This delay was measured to be 308 ms \pm 4 ms.

269 Figure 1 C shows the architecture of the system. Each VR-box contains two Raspberry Pi 3
270 model B connected to a gigabit switch. One is connected to the camera and is only responsible
271 for streaming video. The other, connected to display and speaker, is responsible for playback of
272 sound and image. A third Raspberry Pi 3 is placed on top of the cage responsible for polling the
273 perch sensor at 20 Hz and emitting state changes as events. It also measures temperature and
274 humidity in the box and emits those as events every minute. The multi-channel microphone array
275 is placed outside the isolator box with a microphone placed in each cage. All computers on the
276 network are synchronised to within milliseconds using the Network Time Protocol (*Martin et al.,
277 2010*) implemented with chrony (*Lichvar, 1999*).

278 Data is streamed to IPv6 multi-cast groups following the publish-subscribe pattern (*Birman and
279 Joseph, 1987*). A PC in the bird room acts as historian, saving the data streams. Data is offloaded
280 to a Ceph (*Weil et al., 2006*) persistent storage cluster placed in our data centre. Several event pro-
281 cessors continuously analyse the data streams, producing events. These are running in a docker
282 swarm (*Merkel, 2014*) cluster also in our data centre.

283 The two-layered architecture is based on data streams and event streams (*Larsen et al., 2021*).
284 An event is an association between a specific time and a specific property, in this case a behaviour.
285 A data stream contains sampled data from sensors such as cameras and microphones while an
286 event stream consists of events produced by data stream processors or by asynchronous sensors
287 such as contacts.

288 The continuous audio stream is analysed online to produce the power and entropy events.
289 This analysis is based on estimating the power by squaring the sample values and the entropy as
290 the ratio of the geometric mean to the arithmetic mean. The analysis is implemented as plug-ins
291 to the media-streaming framework *gstreamer* (*Gstreamer, 2001*). The estimates are thresholded
292 with hysteresis (*Larsen et al., 2021*) and published as kafka events (*Vohra, 2016*). A perch sensor
293 installed in the cage directly generates a perch event every time the bird changes location in the
294 cage. Based on those three events, three complex events are generated, namely bout, contact and
295 directed song. The bout event is active when both power and entropy events are active, and the
296 contact event is active when both birds are perched in front of the screen. The directed song event
297 is active when the bout and contact events are active (Fig 1D). Event processing was implemented
298 as microservices in docker containers (*Merkel, 2014*) for high modularity and was running in our
299 data centre.

300 **Animals and husbandry**

301 Adult male and female zebra finches (*Taeniopygia guttata*) were kept pairwise in breeding cages at
302 the University of Southern Denmark, Odense, Denmark on a 12 h light:dark photoperiod and given
303 water and food ad libitum. All experiments were conducted in accordance with the Danish law
304 concerning animal experiments and protocols were approved by the Danish Animal Experiments
305 Inspectorate (Copenhagen, Denmark).

306 We used adult zebra finches (> 100 days post hatch) that were established breeding pairs (mean-
307 ing that they had produced at least one clutch of offspring together) in the animal-animal com-
308 munication experiments and additionally also single males for the animal-computer experiments.
309 When not in experiment, the birds were kept pairwise in breeding cages or in aviaries containing
310 hundreds of individuals. Under experiment the birds were isolated in sound-attenuated boxes
311 for a maximum of ten days before returning to their usual surroundings. The birds had access to
312 food and fresh water ad libitum served at the bottom of the cage and from feeders at the side of
313 the cage. In the VR setup, the birds were kept on a 12 h light:dark photoperiod. The temperature
314 was kept between 22 and 28 °C and the relative humidity at 50-60 %. The temperature difference
315 between the position in front of the screen (front perch) and behind the blind (back perch) was
316 measured with the system fully on to be 0.4 °C (± 0.3 % accuracy). The isolator boxes attenuated
317 sounds in the 200–8,000 Hz range by 40dB (measured by playing back sound in the isolator and
318 record sound levels both inside and outside the box. A fan ensured air flow in the box and provided
319 cooling for the equipment located inside.

320 **Sound segmentation**

321 Segmentation was based on the silence between syllables and was calculated from the amplitude
322 of the signal (Fig 4B). We used two threshold values for discriminating between sound and silence.
323 The input signal (Fig 4A) was normalised to range [-1;1] but otherwise not pre-processed. Starting
324 from the i_{on} th sample where the absolute value of the sample s_i surpasses the on-threshold t_{on} (0.5)

$$i_{on} : |s_i| > t_{on} \quad (1)$$

325 we searched backwards in time to find the onset sample number i_{onset} defined as the sample
326 where the peak-to-peak amplitude over w samples (325) was below the off-threshold t_{off} (0.5).

$$i_{onset} : \max(s_{i-w} : s_i) - \min(s_{i-w} : s_i) < t_{off} \quad (2)$$

327 Similarly we searched for the offset sample number i_{offset} as new samples arrived.

$$i_{offset} : \max(s_i : s_{i+w}) - \min(s_i : s_{i+w}) < t_{off} \quad (3)$$

328 As soon as the last sample was received the segment was passed on to the next stage of the
329 pipeline. Segments shorter than 30 ms or longer than 300 ms were discarded since the duration
330 of zebra finch syllables is expected to be within that range. We implemented both an online and
331 offline version of this segmentation algorithm and used it for all the experiments presented in this
332 paper.

333 **Perch preference protocol**

334 The same data was used for all the animal-animal communication experiments. The VR-setup was
335 powered down for at least 2 hours before the birds were moved to the isolator box (day 0) and left
336 off for at least 24 hours before it was turned on for another full day (day 1). Experiments ran on the
337 following days starting when the cage lights were turned on and for two hours thereafter. Day 2
338 was always with black screen and no sound and the following days the system cycled through per-
339 turbations of two speaker states (off, on) and two screen states (off, on) in randomised order. After
340 the experiments the birds were returned to their home cages. To investigate the motivation for
341 using the VR setup, we looked at the perch preference in different states of the system. Based on
342 the perch sensor, an event was emitted every time the bird changed position in the cage and sum-
343 ming the duration of the events gives a measure of the proportion of time spent in each position
344 (Fig 1E).

345 **Call-timing protocol**

346 The audio was segmented as described above and combined into one big dataset covering 12 hours
347 a day for all 12 pairs. To provide training data, we then hand-annotated for each bird the first
348 30 minutes with both video and audio on. To ease annotation, we used pre-clustering based
349 on cross-correlation, so the observer was presented with oscillograms, spectrograms and sound
350 from one minute at a time that had already been clustered into groups of sounds with high cross-
351 correlation maximum. The observer then had to name the groups and correct mistakes made by
352 the pre-clustering algorithm. The classes found were song, stack calls, distance calls, echo (loud
353 sounds from the other bird triggering the segmentation), wing flapping and noise. Classification of
354 vocalisations followed the descriptions in *Zann (1996)*. Based on the annotations a random forest
355 classifier (*Breiman, 2001*) with 100 estimators was trained for each bird ranging in mean accuracy
356 (10 % hold out) from 0.82 to 0.96. To investigate call timing, we measured the time difference from
357 the playback of a stack call (onset + delay) to the next stack call emitted by the animal of interest
358 up to a maximum of 2 seconds. Histogram of the time differences were constructed (200 bins) and
359 plotted with Gaussian Kernel Density Estimates (KDE, bandwidth=100, fig 2B).

360 **Directed song protocol**

361 To confirm directed song in the animal-animal communication experiments, we selected videos
362 with potential female directed song based on the definition that both birds were on the front perch
363 and the male was vocalising. The videos were then scored by experienced observers (IA, CPHE)
364 for the display of hopping, jumping, beak wiping, looking at the mate and fluffing plumage (see
365 figure 3D for examples). As a quantitative measure, we calculated the coefficient of variance of
366 the fundamental frequency, which is lower in DS compared to US (*Kao et al., 2005*). However, this
367 measure is extracted from stack syllables without frequency modulation such as the one shown
368 in figure 3B. The motif of five birds contained a suitable syllable. From spectrograms of the motifs
369 identified by the online motif detector, we manually selected the same place in the stack syllable
370 (Fig 3B) in 30 motifs from each individual. The fundamental frequency was estimated from 2048
371 (42 ms) samples using the YIN algorithm (*De Cheveigné and Kawahara, 2002*).

372 **Animal-computer communication experiments**

373 For the driving experiments, the male was left to habituate to the new surroundings until he pro-
374 duced at least 10 motif repetitions during the first two hours after lights on (day 0). On the fol-
375 lowing day (day 1) we ran the driving experiment, meaning that videos were displayed showing
376 excited females. Three videos of different females were used, each one minute long, taken from
377 the animal-animal communication experiments. In case of pair-bonded males, the established
378 mates of the focal animals were not among the female videos. In case of single males the 60,000
379 training samples were recorded over three days prior to the experiment. The logic of the system
380 is that every time a motif is detected, a timer is reset. If the timer ran out (3 minutes since last
381 motif) the next video was displayed and otherwise the same video kept getting looped. On day 2
382 we recorded the control without video playbacks.

383 **Online motif detector**

384 The feature extraction is based on summing the rows and columns of the spectrogram (Fig 4D) and
385 concatenating them to form a feature vector (Fig 4E).

386 First a spectrogram of the segment is formed by applying Short-Time Fourier Transform (STFT)
387 with FFT size of 1440 and stride of 25 samples. The parameters are all based on the sampling
388 frequency of 48 kHz, the duration of sounds (30-300 ms) and the desired number of time bins. The
389 smallest spectrogram we can make has just one time bin and thus the maximum FFT size is:

$$FFT = 30ms * 48kHz = 1440bins \quad (4)$$

390 The stride parameter can then be calculated:

$$stride = ((300ms * 48kHz) - 1440bins) / 512bins = 25.3125 \approx 25 \quad (5)$$

391 The spectrogram is cropped to the approximate audible range for zebra finches 200 Hz to 8 kHz
392 (234 bins) and the time dimension is cropped to the first 512 time bins corresponding to 300 ms
393 (zero-padded if the segment duration is shorter). The rows and columns of the spectrogram are
394 summed and the two resulting vectors F_t and F_f are concatenated to form a 746-dimensional
395 feature vector F (Fig 4E).

$$F_t = \sum_t STFT(t, f) \quad (6)$$

396

$$F_f = \sum_f STFT(t, f) \quad (7)$$

397

$$F = [F_t \ F_f] \quad (8)$$

398 Each vector is normalised to have a sum of one before concatenation.

399 A training set is created consisting of 60,000 feature vectors from the same individual, each
400 representing one sound segment. We embed each of these high-dimensional points in a two-
401 dimensional space (Fig 4F) using the t-SNE method introduced in *Maaten and Hinton (2008)*. The
402 method minimises the relative entropy between two distributions, one representing the high-di-
403 mensional points and one representing the low-dimensional points, so that close points in the
404 high-dimensional space are also close in the low dimensional space.

405 Since we are interested in stereotyped behaviour, we then loosely follow the method described
406 in Berman et al. (2014) placing a Gaussian kernel (bandwidth=15) on each embedded point we
407 generate a density plot (Fig 4G), and we find all peaks that are separated by a distance of 15 or
408 more. Using the watershed algorithm (*Meyer, 1994*) on the inverted density plot, we get a set of
409 clusters, each representing roughly a stereotyped syllable. Examples from three different regions
410 can be seen in figure 4G. The further a point is from the peak of the region the more likely it is to be
411 mis-classified and thus distance from peak could be used to indicate certainty of the classification.

412 We found that some regions represent a merge of two syllables while some represent part of a
 413 split syllable. For higher accuracy in detecting the syllables this information could be used for post
 414 processing or better means of segmentation could be introduced.

415 After the training phase a new data point z is embedded based on the already embedded points,
 416 largely using the method described in **Berman et al. (2014)** appendix D. The perplexity parameter of
 417 the t-SNE algorithm can be interpreted as a measure of the number of nearest neighbours (**Maaten
 418 and Hinton, 2008**) and therefore we only consider the 'perplexity' nearest points X in the high
 419 dimensional space found using the ball tree algorithm (**Omohundro, 1989**).

420 We then choose an embedding z' of the new point z such that conditional probabilities in the
 421 low-dimensional space $q_{j|z'}$ are similar to those in the high-dimensional space $p_{j|z}$. The conditional
 422 probability of a point $x_j \in X$ given the new point z is:

$$p_{x_j|z} = \frac{D_{KL}(z||x_j)^2/2\sigma_z^2}{\sum_{x \in X} D_{KL}(z||x)^2/2\sigma_z^2} \quad (9)$$

423 where X is the vector of nearest points in the high-dimensional space, z is the new point in the
 424 high-dimensional space, sigma is found by a binary search for the value that produces a conditional
 425 probability with the perplexity set by the user and D_{KL} is the relative entropy given by:

$$D_{KL}(P||Q) = \sum_{x \in X} P(x) \log \left(\frac{P(x)}{Q(x)} \right) = - \sum_{x \in X} P(x) \log \left(\frac{Q(x)}{P(x)} \right) \quad (10)$$

426 The conditional probability of a point x'_j in the low-dimensional embedding X' given the new
 427 embedding z' :

$$q_{j|z'} = \frac{(1 + \Delta_{j,z'}^2)^{-1}}{\sum_{x' \in X'} (1 + \Delta_{x',z'}^2)^{-1}} \quad (11)$$

428 where $\Delta_{a,b}$ is the euclidean distance between the points a and b . Since z' is the only unknown,
 429 we can find it by minimising $-D_{KL}(p_{x|z}||q_{x'|z'})$

$$z' = \arg \min_{z'} (-D_{KL}(p_{x|z}||q_{x'|z'})) \quad (12)$$

430 using the Nelder-Mead simplex algorithm (**Nelder and Mead, 1965**) and a start guess being the
 431 centroid of the embedding X' of the nearest points X . If the start guess is not in the basin of
 432 attraction of the global minimum, it means that the new point is not like any points presented
 433 during training and the embedded point will shoot towards infinity (**Berman et al., 2014**).

434 One instance of the segmentation algorithm was running for each of the two audio channels
 435 used in the experiment and a new feature vector was formed for each detected segment and
 436 placed in a queue. A pool of 6 workers (containers running in the cluster) processed feature vec-
 437 tors from the queue using the post-embedding algorithm described above and emitted events
 438 containing onset, bird ID, the low dimensional point, a letter representing the region it belonged
 439 to and the latency measured from the end of the segment until the event was emitted. The me-
 440 dian latency over 3 million syllables was 1.089 s (percentiles: 5th=0.356, 25th=0.945, 75th=1.304,
 441 95th=2.500). We found that 95 % of the segments were classified and the remaining 5 % were
 442 marked as unclassified.

443 Sequence events were generated, by event-processors in the cluster, based on the timing of
 444 the syllable events. If the onset of the next segment was within a window of 0.5 s after the offset
 445 of the previous, it was added to the sequence and otherwise it was assigned to a new sequence.
 446 Within 3 s after the end of a sequence an event was emitted containing onset, offset, bird id and
 447 the sequence.

448 To find the motif of the bird we formed a transition probability matrix based on the training
 449 data. Since the transitions in the motif were by far the most frequent, the syllables in the motif
 450 already stood out. Because the motif was repeated several times in a bout, they formed cycles

451 in the transition matrix (Fig 4H). We found the cycle by starting from the globally most frequent
452 transition and following the locally most frequent transitions until getting back to an already visited
453 element. If the motif contained repeated syllables or if the bird sang a lot of introductory notes,
454 there was a possibility for dead ends, but they could be detected and solved programmatically.

455 The birds often sing variations of the long motif so we found the ten most common substrings
456 of the motif and looked for those in the sequence events. We counted the number of occurrences
457 of each substring in the sequence and if a motif was present, we emitted a motif event (based
458 on the most frequent substring in the sequence) containing onset, motif, number of occurrences
459 and bird id. The motif detector was implemented as an event-processor running in the cluster. To
460 verify the motif detector, an observer (LBL) looked at the spectrograms of all the motifs generated
461 online during the two hours of experimentation for one bird (96 motifs) and confirmed that all of
462 them were indeed motifs.

463 References

- 464 **Adret P.** Discrimination of video images by zebra finches (*Taeniopygia guttata*): Direct evidence from song
465 performance. *Journal of Comparative Psychology*. 1997; 111(2):115.
- 466 **Ahrens MB,** Li JM, Orger MB, Robson DN, Schier AF, Engert F, Portugues R. Brain-wide neuronal dynamics
467 during motor adaptation in zebrafish. *Nature*. 2012; 485(7399):471–477.
- 468 **Andreassen T,** Surlykke A, Hallam J. Semi-automatic long-term acoustic surveying: A case study with bats.
469 *Ecological Informatics*. 2014; 21:13–24.
- 470 **Anisimov VN,** Herbst JA, Abramchuk AN, Latanov AV, Hahnloser RH, Vysotski AL. Reconstruction of vocal
471 interactions in a group of small songbirds. *nature methods*. 2014; 11(11):1135.
- 472 **Benichov JI,** Benezra SE, Vallentin D, Globerson E, Long MA, Tchernichovski O. The forebrain song system
473 mediates predictive call timing in female and male zebra finches. *Current Biology*. 2016; 26(3):309–318.
- 474 **Benichov JI,** Vallentin D. Inhibition within a premotor circuit controls the timing of vocal turn-taking in zebra
475 finches. *Nature communications*. 2020; 11(1):1–10.
- 476 **Berman GJ,** Choi DM, Bialek W, Shaevitz JW. Mapping the stereotyped behaviour of freely moving fruit flies.
477 *Journal of The Royal Society Interface*. 2014; 11(99):20140672.
- 478 **Birman K,** Joseph T. Exploiting virtual synchrony in distributed systems. *ACM SIGOPS Oper Syst Rev*. 1987;
479 21(5):123–138. doi: [10.1145/37499.37515](https://doi.org/10.1145/37499.37515).
- 480 **Bonnet F,** Kato Y, Halloy J, Mondada F. Infiltrating the zebrafish swarm: design, implementation and exper-
481 imental tests of a miniature robotic fish lure for fish–robot interaction studies. *Artificial Life and Robotics*.
482 2016; 21(3):239–246.
- 483 **Breiman L.** Random forests. *Machine learning*. 2001; 45(1):5–32.
- 484 **Brumm H,** Slabbekoorn H. Acoustic communication in noise. *Advances in the Study of Behavior*. 2005; 35:151–
485 209.
- 486 **Carouso-Peck S,** Goldstein MH. Female social feedback reveals non-imitative mechanisms of vocal learning in
487 zebra finches. *Current Biology*. 2019; 29(4):631–636.
- 488 **Chen Y,** Matheson LE, Sakata JT. Mechanisms underlying the social enhancement of vocal learning in songbirds.
489 *Proceedings of the National Academy of Sciences*. 2016; 113(24):6641–6646.
- 490 **Cong L,** Wang Z, Chai Y, Hang W, Shang C, Yang W, Bai L, Du J, Wang K, Wen Q. Rapid whole brain imaging of
491 neural activity in freely behaving larval zebrafish (*Danio rerio*). *Elife*. 2017; 6:e28158.
- 492 **Cugola G,** Margara A. Processing flows of information: From data stream to complex event processing. *ACM*
493 *Computing Surveys (CSUR)*. 2012; 44(3):1–62.
- 494 **Davidson GL,** Clayton NS. New perspectives in gaze sensitivity research. *Learning & Behavior*. 2016; 44(1):9–17.
- 495 **De Cheveigné A,** Kawahara H. YIN, a fundamental frequency estimator for speech and music. *The Journal of*
496 *the Acoustical Society of America*. 2002; 111(4):1917–1930.

- 497 **Dombeck DA**, Reiser MB. Real neuroscience in virtual worlds. *Current opinion in neurobiology*. 2012; 22(1):3–
498 10.
- 499 **Elie JE**, Mariette MM, Soula HA, Griffith SC, Mathevon N, Vignal C. Vocal communication at the nest between
500 mates in wild zebra finches: a private vocal duet? *Animal Behaviour*. 2010; 80(4):597–605.
- 501 **Elie JE**, Theunissen FE. The vocal repertoire of the domesticated zebra finch: a data-driven approach to decipher
502 the information-bearing acoustic features of communication signals. *Animal cognition*. 2016; 19(2):285–315.
- 503 **Emmerton J**. Pattern discrimination in the near-ultraviolet by pigeons. *Perception & psychophysics*. 1983;
504 34(6):555–559.
- 505 **Galoch Z**, Bischof HJ. Zebra finches actively choose between live images of conspecifics. *Ornithological Science*.
506 2006; 5(1):57–64.
- 507 **Galoch Z**, Bischof HJ. Behavioural responses to video playbacks by zebra finch males. *Behavioural Processes*.
508 2007; 74(1):21–26.
- 509 **Grosenick L**, Marshel JH, Deisseroth K. Closed-loop and activity-guided optogenetic control. *Neuron*. 2015;
510 86(1):106–139.
- 511 **Gstreamer**, GStreamer; 2001. Accessed: 2018-08-28. <https://gstreamer.freedesktop.org/>.
- 512 **Halloy J**, Sempo G, Caprari G, Rivault C, Asadpour M, Tâche F, Saïd I, Durier V, Canonge S, Amé JM, et al.
513 Social integration of robots into groups of cockroaches to control self-organized choices. *Science*. 2007;
514 318(5853):1155–1158.
- 515 **Harvey CD**, Collman F, Dombeck DA, Tank DW. Intracellular dynamics of hippocampal place cells during virtual
516 navigation. *Nature*. 2009; 461(7266):941–946.
- 517 **Hoffmann LA**, Kelly CW, Nicholson DA, Sober SJ. A lightweight, headphones-based system for manipulating
518 auditory feedback in songbirds. *JoVE (Journal of Visualized Experiments)*. 2012; (69):e50027.
- 519 **Ikebuchi M**, Okanoya K. Male zebra finches and Bengalese finches emit directed songs to the video images of
520 conspecific females projected onto a TFT display. *Zoological Science*. 1999; 16(1):63–70.
- 521 **Jarvis ED**, Scharff C, Grossman MR, Ramos JA, Nottebohm F. For whom the bird sings: context-dependent gene
522 expression. *Neuron*. 1998; 21(4):775–788.
- 523 **Kao MH**, Doupe AJ, Brainard MS. Contributions of an avian basal ganglia-forebrain circuit to real-time modu-
524 lation of song. *Nature*. 2005; 433(7026):638–643.
- 525 **Kaupert U**, Thurley K, Frei K, Bagorda F, Schatz A, Tocker G, Rapoport S, Derdikman D, Winter Y. Spatial cog-
526 nition in a virtual reality home-cage extension for freely moving rodents. *Journal of neurophysiology*. 2017;
527 117(4):1736–1748.
- 528 **Klein BA**, Stein J, Taylor RC. Robots in the service of animal behavior. *Communicative & integrative biology*.
529 2012; 5(5):466–472.
- 530 **Kollmorgen S**, Hahnloser RH, Mante V. Nearest neighbours reveal fast and slow components of motor learning.
531 *Nature*. 2020; 577(7791):526–530.
- 532 **Kopman V**, Laut J, Polverino G, Porfiri M. Closed-loop control of zebrafish response using a bioinspired robotic-
533 fish in a preference test. *Journal of the Royal Society Interface*. 2013; 10(78):20120540.
- 534 **Larsen LB**, Neerup MM, Hallam J. Online computational ethology based on modern IT infrastructure. *Ecological*
535 *Informatics*. 2021; 63:101290.
- 536 **Lichvar M**, Chrony; 1999. Accessed: 2020-12-09. <https://chrony.tuxfamily.org/>.
- 537 **Ljubičić I**, Bruno JH, Tchernichovski O. Social influences on song learning. *Current Opinion in Behavioral*
538 *Sciences*. 2016; 7:101–107.
- 539 **Lohr B**, Wright TF, Dooling RJ. Detection and discrimination of natural calls in masking noise by birds: estimating
540 the active space of a signal. *Anim Behav*. 2003 apr; 65(4):763–777. [http://linkinghub.elsevier.com/retrieve/pii/](http://linkinghub.elsevier.com/retrieve/pii/S0003347203920938)
541 [S0003347203920938](http://linkinghub.elsevier.com/retrieve/pii/S0003347203920938), doi: 10.1006/anbe.2003.2093.

- 542 **Maaten Lvd**, Hinton G. Visualizing data using t-SNE. *Journal of machine learning research*. 2008; 9(Nov):2579–
543 2605.
- 544 **de Margerie E**, Lumineau S, Houdelier C, Yris MR. Influence of a mobile robot on the spatial behaviour of quail
545 chicks. *Bioinspiration & Biomimetics*. 2011; 6(3):034001.
- 546 **Marras S**, Porfiri M. Fish and robots swimming together: attraction towards the robot demands biomimetic
547 locomotion. *Journal of The Royal Society Interface*. 2012; 9(73):1856–1868.
- 548 **Martin J**, Burbank J, Kasch W, Mills PDL. Network Time Protocol Version 4: Protocol and Algorithms Specification.
549 RFC Editor; 2010. <https://rfc-editor.org/rfc/rfc5905.txt>, doi: 10.17487/RFC5905. RFC 5905.
- 550 **Merkel D**. Docker: lightweight linux containers for consistent development and deployment. *Linux journal*.
551 2014; 2014(239):2.
- 552 **Meyer F**. Topographic distance and watershed lines. *Signal processing*. 1994; 38(1):113–125.
- 553 **Michelsen A**, Andersen BB, Storm J, Kirchner WH, Lindauer M. How honeybees perceive communication
554 dances, studied by means of a mechanical model. *Behavioral Ecology and Sociobiology*. 1992; 30(3-4):143–
555 150.
- 556 **Nelder JA**, Mead R. A simplex method for function minimization. *The computer journal*. 1965; 7(4):308–313.
- 557 **Nourizonoz A**, Zimmermann R, Ho CLA, Pellat S, Ormen Y, Prévost-Solié C, Reymond G, Pifferi F, Aujard F, Herrel
558 A, et al. EthoLoop: automated closed-loop neuroethology in naturalistic environments. *Nature Methods*.
559 2020; p. 1–8.
- 560 **Nuboer J**, Coemans M, Vos J. Artificial lighting in poultry houses: do hens perceive the modulation of fluorescent
561 lamps as flicker? *British poultry science*. 1992; 33(1):123–133.
- 562 **Omohundro SM**. Five balltree construction algorithms. International Computer Science Institute Berkeley;
563 1989.
- 564 **Partan SR**, Fulmer AG, Gounard MA, Redmond JE. Multimodal alarm behavior in urban and rural gray squirrels
565 studied by means of observation and a mechanical robot. *Current Zoology*. 2010; 56(3):313–326.
- 566 **Partan SR**, Otovic P, Price VL, Brown SE. Assessing display variability in wild brown anoles *Anolis sagrei* using
567 a mechanical lizard model. *Current Zoology*. 2011; 57(2):140–152.
- 568 **Patricelli GL**, Coleman SW, Borgia G. Male satin bowerbirds, *Ptilonorhynchus violaceus*, adjust their display
569 intensity in response to female startling: an experiment with robotic females. *Animal Behaviour*. 2006;
570 71(1):49–59.
- 571 **Polverino G**, Phamduy P, Porfiri M. Fish and robots swimming together in a water tunnel: robot color and
572 tail-beat frequency influence fish behavior. *PloS one*. 2013; 8(10):e77589.
- 573 **Reaney LT**, Sims RA, Sims SW, Jennions MD, Backwell PR. Experiments with robots explain synchronized
574 courtship in fiddler crabs. *Current Biology*. 2008; 18(2):R62–R63.
- 575 **Reiser MB**, Dickinson MH. A modular display system for insect behavioral neuroscience. *Journal of neuro-*
576 *science methods*. 2008; 167(2):127–139.
- 577 **Riedner D**, Adam I. Units of motor production: Bengalese finches interrupt song within syllables. bioRxiv. 2020;
578 <https://www.biorxiv.org/content/10.1101/2020.02.19.956698v1>.
- 579 **Romano D**, Benelli G, Donati E, Remorini D, Canale A, Stefanini C. Multiple cues produced by a robotic fish
580 modulate aggressive behaviour in Siamese fighting fishes. *Scientific reports*. 2017; 7(1):1–11.
- 581 **Rychen J**, Rodrigues DI, Tomka T, Rüttimann L, Yamahachi H, Hahnloser RH. A system for controlling vocal
582 communication networks. *Scientific Reports*. 2021; 11(1):1–15.
- 583 **Simon R**, Varkevisser J, Mendoza E, Hochradel K, Scharff C, Riebel K, Halfwerk W. Development and application
584 of a robotic zebra finch (RoboFinch) to study multimodal cues in vocal communication. *PeerJ Preprints*. 2019;
585 7:e28004v2.
- 586 **So LY**, Munger SJ, Miller JE. Social context-dependent singing alters molecular markers of dopaminergic and
587 glutamatergic signaling in finch basal ganglia Area X. *Behavioural Brain Research*. 2019; 360:103–112.

- 588 **Sober SJ**, Brainard MS. Adult birdsong is actively maintained by error correction. *Nature neuroscience*. 2009;
589 12(7):927.
- 590 **Sossinka R**, Böhner J. Song types in the zebra finch *Poephila guttata castanotis* 1. *Zeitschrift für Tierpsychologie*.
591 1980; 53(2):123–132.
- 592 **Steuer J**. Defining virtual reality: Dimensions determining telepresence. *Journal of communication*. 1992;
593 42(4):73–93.
- 594 **Stowers JR**, Hofbauer M, Bastien R, Griessner J, Higgins P, Farooqui S, Fischer RM, Nowikovsky K, Haubensak
595 W, Couzin ID, et al. Virtual reality for freely moving animals. *Nature methods*. 2017; 14(10):995–1002.
- 596 **Tchernichovski O**, Nottebohm F, Ho CE, Pesaran B, Mitra PP. A procedure for an automated measurement of
597 song similarity. *Animal behaviour*. 2000; 59(6):1167–1176.
- 598 **Ter Maat A**, Trost L, Sagunsky H, Seltmann S, Gahr M. Zebra finch mates use their forebrain song system in
599 unlearned call communication. *PloS one*. 2014; 9(10):e109334.
- 600 **Vohra D**. Apache Kafka. In: *Pract. Hadoop Ecosyst*. Berkeley, CA: Apress; 2016.p. 339–347. http://link.springer.com/10.1007/978-1-4842-2199-0_{_}9, doi: 10.1007/978-1-4842-2199-0_9.
- 602 **Weil SA**, Brandt SA, Miller EL, Long DD, Maltzahn C. Ceph: A scalable, high-performance distributed file system.
603 In: *Proceedings of the 7th symposium on Operating systems design and implementation*; 2006. p. 307–320.
- 604 **Zann RA**. The zebra finch: a synthesis of field and laboratory studies, vol. 5. Oxford University Press; 1996.